

UC Berkeley

UC Berkeley Previously Published Works

Title

The Three Members of the Arabidopsis Glycosyltransferase Family 92 are Functional β -1,4-Galactan Synthases

Permalink

<https://escholarship.org/uc/item/5v02w456>

Journal

Plant and Cell Physiology, 59(12)

ISSN

0032-0781

Authors

Ebert, Berit

Birdseye, Devon

Liwanag, April JM

et al.

Publication Date

2018-12-01

DOI

10.1093/pcp/pcy180

Peer reviewed

Cover page

The Three Members of the Arabidopsis Glycosyltransferase Family 92 are Functional β -1,4-Galactan Synthases

Running Title

Identification of β -1,4-Galactan Synthases in Arabidopsis

Author for correspondence:

H. V. Scheller

Joint BioEnergy Institute, Feedstocks Division

Lawrence Berkeley National Laboratory

5885 Hollis St., 4th floor

Emeryville, CA 94608

Tel.: 510-486-7371 (office)

Fax: 510-486-4252

Email: hscheller@lbl.gov

Subject areas

Proteins, enzymes and metabolism

Structure and function of cells

The submission comprises the main manuscript, 8 figures and 2 tables. Supporting Information comprises 6 Supplemental Figures and 1 supplemental table.

Title page

The Three Members of the *Arabidopsis thaliana* Glycosyltransferase Family 92 are Functional β -1,4-Galactan Synthases

Running Title

Identification of β -1,4-Galactan Synthases in Arabidopsis

Berit Ebert^{1,2,3}, Devon Birdseye¹, April J.M. Liwanag¹, Tomas Laursen¹, Emilie A. Rennie¹, Xiaoyuan Guo², Michela Catena¹, Carsten Rautengarten^{1,3}, Solomon H. Stonebloom¹, Pawel Gluza³, Venkataramana Pidatala¹, Mathias C. F. Andersen⁴, Roshan Cheetamun⁵, Jenny C. Mortimer¹, Joshua L. Heazlewood³, Antony Bacic⁵, Mads H. Clausen⁴, William G.T. Willats² and Henrik V. Scheller*^{1,6}

¹Joint BioEnergy Institute and Biological Systems and Engineering Division, Lawrence Berkeley National Laboratory, Berkeley, California, USA; ²Department of Plant and Environmental Sciences, University of Copenhagen, Frederiksberg, Denmark; ³School of BioSciences, The University of Melbourne, Victoria, Australia; ⁴Center for Nanomedicine and Theranostics, Department of Chemistry, Technical University of Denmark, Kgs. Lyngby, Denmark; ⁵ARC Centre of Excellence in Plant Cell Walls, School of BioSciences, The University of Melbourne, Victoria, Australia; ⁶Department of Plant and Microbial Biology, University of California, Berkeley, California, USA

*Author for correspondence:

Henrik Vibe Scheller

hscheller@lbl.gov

Fax: 510-486-4252

Abstract

Pectin is a major component of primary cell walls and performs a plethora of functions crucial for plant growth, development and plant-defense responses. Despite the importance of pectic polysaccharides their biosynthesis is poorly understood. Several genes have been implicated in pectin biosynthesis by mutant analysis, but biochemical activity has been shown for very few.

We used reverse genetics and biochemical analysis to study members of Glycosyltransferase Family 92 (GT92) in *Arabidopsis thaliana*. Biochemical analysis gave detailed insight into the properties of GALS1 (Galactan synthase 1) and showed galactan synthase activity of GALS2 and GALS3. All proteins are responsible for adding galactose onto existing galactose residues attached to the rhamnogalacturonan-I (RG-I) backbone. Significant GALS activity was observed with galactopentaose as acceptor but longer acceptors are favored. Overexpression of the GALS proteins in *Arabidopsis* resulted in accumulation of unbranched β -1,4-galactan. Plants in which all three genes were inactivated had no detectable β -1,4-galactan, and surprisingly these plants exhibited no obvious developmental phenotypes under standard growth conditions. RG-I in the triple mutants retained branching indicating that the initial Gal substitutions on the RG-I backbone are added by enzymes different from GALS.

Keywords: *Arabidopsis*, cell wall, galactan, glycosyltransferases, galactosyltransferases, pectin, rhamnogalacturonan-I

Abbreviations: AGP, arabinogalactanprotein, AIR, alcohol insoluble residue, Ara, arabinose, CDTA, 1,2-Diaminocyclohexanetetraacetic acid, DP, degree of polymerization, Fuc, fucose, Gal, galactose, GALS, galactansynthase, GT, glycosyltransferase, HG, homogalacturonan, HPAEC-PAD, High performance anion exchange chromatography with pulsed amperometric detection, PACE, Polysaccharide analysis using carbohydrate gel electrophoresis, RG-I, rhamnogalacturonan-I, Rha, rhamnose, RT-PCR, Reverse transcription polymerase chain reaction, WT, wild type, XGA, xylogalacturonan, Xyl, xylose, YFP, yellow fluorescent protein

INTRODUCTION

Pectin is a key component in primary walls of dicots, gymnosperms and non-commelinid monocots, and present in smaller amounts in secondary walls and in primary walls of grasses. Pectin is considered a family of different polysaccharides or glycan domains rather than a single structural polymer. In dicots, like Arabidopsis, pectin constitutes 20% to 35% of the primary wall (Atmodjo et al. 2013; Mohnen 2008). Besides being a structural component of the cell wall, pectic polysaccharides have a multitude of specialized functions. These include processes like cell-cell adhesion (Daher and Braybrook 2015), cell elongation (Dumont et al. 2014), wall porosity, and extensibility that are vital for plant growth (Bidhendi and Geitmann 2016). Furthermore, pectins are a source of signaling molecules with roles in development and disease resistance (Rasul et al. 2012; Ridley et al. 2001) and as a hydration polymer for seed and root growth (Arsovski et al. 2010; Blamey 2003). The highly complex pectic matrix is comprised of four polysaccharide ‘domains’, which are connected through covalent linkages although it is not known that the four domains are present in a single macromolecule. The main domains are homogalacturonan (HG) and rhamnogalacturonan-I (RG-I) while rhamnogalacturonan-II (RG-II) and xylogalacturonan (XGA) are minor components. HG, the most abundant (~65%) and structurally simplest domain, is a linear homopolymer consisting of α -1,4-linked D-galacturonic acid (GalA). The GalA residues in pure galacturonan backbones can be methylesterified at the C6 carboxyl position and/or acetylated at the O-2 or O-3 position (Harholt et al. 2010). In XGA some of the GalA residues of the HG backbone are further decorated with xylose (Xyl) residues at the O-3 position. RG-II, representing ~10% of the pectic domains, is structurally the most complex consisting of an HG backbone with diverse side chains of 13 different sugar types linked to each other by up to 21 different glycosidic linkages in six different sidechains (Ndeh et al. 2017). RG-I typically constitutes ~20-35% of pectin. In contrast to the other domains, which have a backbone consisting solely of GalA, the RG-I backbone contains the repeating disaccharide [-4- α -D-GalA-(1,2)- α -L-Rha-1-]. The rhamnose (Rha) residues of the backbone can be substituted with β -D-Galp residues at the O-4 position that are further substituted with β -1,4-linked Gal or α -L-Araf resulting in various sidechains including β -1,4-galactan, linear and branched arabinans (**Supplementary Figure S1**). Additionally, type I and II-arabinogalactans are attached to Rha residues of the RG-I backbone. Type-I arabinogalactans consist of β -1,4-linked D-Galp backbones with arabinan sidechains, while type-II

arabinogalactans have a backbone of β -1,3-, β -1,6- and β -1,3,6- linked D-Galp similar to the arabinogalactans of Arabinogalactan-proteins (AGPs) (de Vries and Visser 2001).

RG-I shows great variation in the number of sugars, oligosaccharides and oligosaccharide branching within different plant species but also within different cell types and at different developmental stages. What causes this structural variation is unknown, however it likely reflects specific RG-I functions (Mohnen 2008).

Like other complex matrix polysaccharides, pectic polymers are synthesized in the Golgi apparatus by glycosyltransferases (GTs). The current hypothesis suggests that pectins are synthesized, assembled and processed while they move through the Golgi cisternae and the *trans*-Golgi network. Lastly pectins are secreted into Golgi-derived vesicles and transported to the cell surface where further modification/re-modelling occurs upon deposition (Driouich et al. 2012).

Although it has been estimated that more than 67 different transferase activities are required for the assembly of the pectic matrix only a few transferases have been unambiguously identified (Mohnen 2008). The first GT identified playing a role in pectin biosynthesis, specifically HG backbone formation, was the HG galacturonosyltransferase GAUT1 (Sterling et al. 2006). GAUT1 works together with GAUT7, which is not enzymatically active but provides the Golgi anchor for GAUT1 (Atmodjo et al. 2011). More GAUT and GAUT-like (GATL) proteins have been implicated in pectin biosynthesis yet their precise roles and activities need to be established. XYLOGALACTURONAN DEFICIENT 1 (XGD1) has been identified as a xylosyltransferase transferring Xyl onto the HG backbone to generate XGA (Jensen et al. 2008). The complexity of RG-II argues for the requirement of many GTs nonetheless only the RHAMNOGALACTURONAN II XYLOSYLTRANSFERASES (RGXTs) that transfer Xyl onto fucose (Fuc) in RG-II side chain A have been identified (Egelund et al. 2008; Egelund et al. 2006; Jensen et al. 2008; Liu et al. 2011). A putative arabinosyltransferase ARABINAN DEFICIENT1 (ARAD1) was identified studying loss-of-function mutants with significantly decreased amounts of arabinose (Ara) in leaves and stems, originating from arabinan in RG-I (Harholt et al. 2006). However, despite substantial efforts biochemical activity of ARAD1 has yet to be demonstrated. ARAD2, an ARAD1 homolog, has also been implicated in pectic arabinan biosynthesis. However, *arad2* and *arad1/arad2* mutants revealed that the genes are not functionally redundant (Harholt et al. 2012).

We have previously reported the identification of the β -1,4-galactan galactosyltransferase GALACTAN SYNTHASE 1 (GALS1) in *Arabidopsis* (Liwanag et al. 2012). β -1,4-galactan is mainly found as side chains of RG-I in primary walls, and is also present in secondary walls of trees forming reaction wood in response to gravitropic stimuli (Du and Yamamoto 2007). Conifers including *Pinus radiata* react when exposed to a gravitational stimulus by producing compression wood, which in contrast to normal wood has significant amounts of β -1,4-galactan (Mast et al. 2009). In angiosperm trees like *Populus spp.* galactans are found in the non-lignified fiber cells (gelatinous fibers) of tension wood (Arend 2008; Gorshkova et al. 2015). These specialized fiber cells possess an inner gelatinous cell-layer called the G-layer and besides in stems they can be found in various plant organs and in both phloem and xylem (Mellerowicz and Gorshkova 2012). Extraxylary gelatinous fibers are present in the stems of major fiber crops including hemp and flax and based on their characteristics can be grouped together with tension wood fibers (Gorshkova and Morvan 2006; Mellerowicz and Gorshkova 2012).

GALS1, along with its two homologs are members of Glycosyltransferase Family 92 (GT92) (Hansen et al. 2012; Titz et al. 2009), of which all members contain a DUF23 motif. The existence of β -1,4-galactan galactosyltransferase activity in plants was established 50 years ago (McNab et al. 1968) and synthesis of β -1,4-galactan in different plant species has been demonstrated in multiple *in vitro* studies (Atmodjo et al. 2013). However, only recently were we able to show that purified recombinant GALS1 protein can use UDP-Gal as donor substrate to elongate the β -1,4-galactopentaose that was provided as acceptor and that GALS1 functions as β -1,4-galactan galactosyltransferase *in vitro* and *in vivo* (Liwanag et al. 2012). More recently, GALS1 was shown to also have arabinopyranosyl-transferase activity; it can add arabinopyranose to the end of growing galactan chains thereby preventing their further elongation (Laursen et al. 2018).

In this study, we investigated and compared the biochemical function of all three members of GT92. Furthermore, we studied the result of inactivating all three genes on pectin structure and plant growth.

RESULTS

The Three GALS Proteins Localize to the Golgi Apparatus

To establish the sub-cellular localizations of the GALS2 and GALS3 proteins we generated N-terminal Yellow Fluorescent Protein (YFP) fusions and transiently co-expressed these together with the Golgi marker α -mannosidase 1 (Nelson et al. 2007) in *N. benthamiana*. Similarly to GALS1, the GALS2 and GALS3 proteins localized to Golgi-like punctate structures and co-localized with the Golgi marker protein (**Figure 1**) consistent with a role in pectin biosynthesis.

GALS 1, 2 and 3 Elongate β -1,4-Galactans

Microsomal membrane preparations containing GALS1 as well as the purified GALS1 protein have the capability to transfer Gal onto a β -1,4-galactopentaose acceptor when UDP- $[^{14}\text{C}]\text{Gal}$ was present in the reaction mixture (Liwanag et al. 2012). To optimize the conditions used to assay galactan synthase activity, we initially tested how various co-factors and pH values affect the activity of the recombinant and purified GALS1 protein. A preference for Mn^{2+} over Mg^{2+} has been shown in our previous study however the optimum was not determined (Laursen et al. 2018). We here tested a wider range of divalent cation concentrations and found an optimum at 20 mM Mn^{2+} , while neither Mg^{2+} nor Co^{2+} could substitute at any concentration tested (**Figure 2**). The enzyme had a pH optimum of 6.0-6.5, consistent with the pH of the Golgi lumen.

To further characterize the GALS1 activity, we used chemically synthesized linear and branched galacto-oligosaccharides and arabinogalactans as acceptors (**Figure 3a**). The activity assays were performed with UDP- $[^{14}\text{C}]\text{Gal}$ and the different β -1,4-D-galacto-oligosaccharides as acceptor substrates, using affinity-purified FLAG-GALS1. As control we used protein extracted from plants only expressing the p19 gene from the *Tomato bushy stunt virus* to suppress gene silencing (Qu and Morris 2002). Unincorporated radiolabel was removed by chromatography through an anion-exchange column and the labeled products were measured by scintillation counting. The β -1,4-GalT assays revealed that FLAG-GALS1 fusion protein extracts had activity when a β -1,4-galactooligomer with a length of at least four was provided as acceptor substrate (**Figure 3b**). However, no significant activity compared to the p19 control was observed when shorter acceptors such as Gal, galactobiose or galactotriose were used in the assays. Interestingly, the observed β -1,4-GalT activity increased concomitantly with the length of the provided acceptors as an increased β -1,4-GalT activity was detected when galactopentaose, galactohexaose and galactoheptaose were used

as acceptors in the assay (compound 5 to 7). Since no longer β -1,4-galacto-oligosaccharide acceptors were available as substrates for β -1,4-GalT assays, it cannot be excluded that longer acceptors would have higher β -1,4-GalT activity, though the data suggest that the activity levels off by DP six to seven. We also tested the β -1,4-GalT activity when branched acceptors were added to the assay mixture. GALS1 did not show substantial activity when decorated galacto-oligosaccharides were used as substrates (**Figure 3b**, compound 8 to 12). This demonstrates that GALS1 prefers linear β -1,4-linked galactans for proper function.

To investigate whether GALS2 and GALS3 behave similar to GALS1, we transiently overexpressed all three proteins fused to YFP by infiltrating leaves of *N. benthamiana* with *Agrobacterium tumefaciens* (Agrobacterium) carrying the respective construct. From infiltrated leaves, microsomes were prepared and subsequently used for activity assays. Initially, we used the microsomal preparations to test the attachment of Gal onto endogenous acceptors in the presence of UDP- ^{14}C Gal. Microsomal preparations from plants overexpressing either the GALS1, GALS2 or GALS3 protein showed increased galactan synthase activity over the endogenous activity of microsomal preparations from plants expressing only the p19 protein (**Figure 4a**). Whereas with GALS1 microsomes an increase of more than fifteen-fold over the p19 control was detected, GALS2 and GALS3 microsomes showed increased activity of about five and three times, respectively. To assess the protein expression in the microsomal preparations we performed an immunoblot analysis, which showed considerable variation in GALS protein abundance in the microsomal preparations (**Figure 4b**). YFP-GALS1 was expressed at much higher levels than the two other proteins, and therefore the difference in activity between the three proteins could be due to different expression levels. Although, we attempted expressing the three GALS proteins in *N. benthamiana* numerous times we consistently found that GALS2 and GALS3 express poorly or accumulate to much lower levels than GALS1. To tackle this problem we used microsomal protein fractions obtained from transgenic Arabidopsis plants for *in vitro* GalT assays and detected the reaction products by PACE (Goubet et al. 2002). Compared to *N. benthamiana*, Arabidopsis microsomal preparations produce only little background allowing enzymatic assays without extensive protein purification (**Figure 5**). The application of the PACE assay confirmed our results from activity assays with microsomes isolated from *N. benthamiana* plants transiently expressing the GALS proteins that established galactosyltransferase activity

with endogenous acceptors. Even when the amount of enzyme in the assays was normalized, GALS1 still showed higher activity than GALS2 and GALS3 (**Figure 5c**).

GALS 1, 2 and 3 Contribute to Galactan Biosynthesis in vivo

We have identified homozygous *gals1*, *gals2* and *gals3* mutants and shown that these have decreased levels of total cell wall Gal compared to the WT (Liwanag et al. 2012). However, none of the single mutants showed obvious morphological abnormalities compared to the WT (**Supplementary Figure S2**). Since all three GT92 proteins were able to elongate β -1,4-D-galacto-oligosaccharides and single mutants displayed the same biochemical phenotype it seemed likely that they might function in similar ways *in planta*. To explore that in more detail we generated double mutants by crossing *gals1-1* with *gals2-1*, *gals1-1* with *gals3-1* and *gals2-1* with *gals3-1*. We then generated a triple mutant by crossing the *gals1-1/gals3-1* and the *gals2-1/gals3-1* double mutants. The mutant genotypes were confirmed by amplification of the full-length transcript using RT-PCR (**Supplementary Figure S3**). To further assess if the loss of transcript of either one or multiple *GALS* genes affects the transcript abundance of the remaining family members we performed quantitative RT-PCR (**Supplementary Figure S4**). The *gals1-1*, *gals2-1* and *gals3-1* single mutants were analyzed for comparison. The quantitative RT-PCR data confirmed a substantial decrease of *GALS1* expression and the lack of *GALS2* and *GALS3* transcripts in all of the mutants (**Supplementary Figure S4**). There was no indication of a compensatory increase in expression of the non-mutated gene(s) in any of the mutants; if anything, the transcript abundance of the non-mutated *GALS* genes was slightly reduced compared to the WT (**Supplementary Figure S4**).

Remarkably, the loss or significant down-regulation of the transcripts of all three *GALS* genes did not have an obvious impact on the morphological or developmental phenotypes of these plants since we could not observe any differences in comparison to the WT with regard to bolting time, rosette size or stem height (**Supplementary Figure S2**). To explore if morphology or development are affected when the mutant plants are subjected to certain stress conditions, we tested growth responses upon osmotic stress and treatment with the actin disruptor Latrunculin B and the cellulose inhibitor isoxaben. However none of the stresses investigated led to an altered response of the mutants compared to the wild type (**Supplementary Figure S5**).

To investigate biochemical changes in *gals* mutant cell walls, we extracted AIR and analyzed the monosaccharide composition. All mutants revealed a significant decrease in total cell wall Gal, with the largest reductions in double and triple mutants (**Table 1**). To explore the changes in mutant cell walls in more detail we performed immunodot blot analyses using the LM5 antibody, which specifically recognizes more than three contiguous units of 1,4- β -galactosyl residues (Andersen et al. 2016a; Jones et al. 1997). The analysis revealed no binding of the LM5 antibody when cell wall preparations derived from the *gals2/gals3* double and the *gals1/gals2/gals3* triple mutant were spotted on the membrane (**Figure 6a**). As a control for equal loading we tested binding of the LM19 antibody, which specifically recognizes HG epitopes (Verhertbruggen et al. 2009), and as expected there was no difference in signal intensity observable between the different mutants (**Figure 6b**). The result that the LM5 epitope is not recognized in cell wall material extracted from the *gals2/gals3* double mutant and the triple mutant indicates that without the GALS proteins no elongated β -1,4-galactans can be synthesized. We do not have an explanation why the *gals2/gals3* double mutant differs from the other double mutants, but this result was consistently observed.

To investigate alterations in the triple mutant and the GALS1 overexpression line in further detail we performed microarray polymer profiling on cell wall material isolated from plants grown in liquid culture (**Figure 6c**). Microarray polymer profiling analysis confirmed that no binding of the LM5 antibody was detectable when cell wall preparations derived from the *gals1/gals2/gals3* triple mutant were spotted onto the array. In contrast, LM5 binding was significantly increased when cell wall material from the GALS1 overexpression line was compared to that from the WT (**Figure 6c**). In addition, we used an array of cell wall polysaccharide specific antibodies to test if the loss or accumulation of elongated β -1,4-galactans leads to changes in other wall polymers. While no major differences could be observed in CDTA extracted samples using antibodies recognizing different HG epitopes (JIM5, JIM7, LM18, LM19) (Clausen et al. 2003; Verhertbruggen et al. 2009) and an epitope found in AGPs (JIM13) (Knox et al. 1991), slightly reduced binding was detected in both the triple mutant and the GALS1 overexpression line with antibodies against epitopes of the RG-I backbone (RU1, RU2) (Ralet et al. 2010) as well as 1,5- α -arabinan (LM6) (Willats et al. 1998) found in RG-I sidechains. In samples subjected to a second extraction step with NaOH, small differences between the mutant and the WT were observed with antibodies directed

against xylan epitopes (LM11, AX1) (Guillon et al. 2004; McCartney et al. 2005). No change was seen when labeling was performed with LM25, an antibody that detects a xyloglucan epitope (Pedersen et al. 2012). In contrast, slightly less labeling was observed in the triple mutant compared to GALS1 overexpressor and WT when the cellulose-binding module 3a (Blake et al. 2006) was used (**Figure 6c**). These results indicate that minor changes in the composition of other wall polymers occur when Arabidopsis RG-I β -1,4-galactan content is modulated.

Overexpression of GALS Genes Causes Accumulation of Cell Wall Gal Specifically as 1,4-Linked β -Galactan

Arabidopsis plants stably transformed with a *35S:YFP-GALS1* fusion construct contained significantly more cell wall Gal compared to WT plants, underpinning the function of GALS1 as galactan synthase. To test if GALS2 and GALS3 function in a comparable manner we placed both genes under the control of the 35S promoter from the Cauliflower Mosaic Virus, stably transformed these constructs into Arabidopsis and analyzed the monosaccharide composition of the resultant transgenic lines. Similar to what was observed for plants overexpressing *GALS1*, plant lines overexpressing *GALS2* and *GALS3* accumulated significantly more Gal in rosette leaves than WT plants (**Figure 7**). The Gal levels in the strongest overexpression lines were comparable for all three genes and most of the lines contained up to 50% more cell wall Gal than the WT (**Figure 7a**). To analyze whether the additional Gal in these overexpression lines was deposited as β -1,4-galactan we performed a digest with an endo- β -1,4-galactanase from *A. niger*. For all three overexpression lines (*GALS1* was tested as control) almost all of the extra Gal could be released by the endo- β -1,4-galactanase (**Figure 7b**). This result strongly indicates that like *GALS1*, both *GALS2* and *GALS3* function as β -1,4-galactan synthases *in vivo*.

Loss-of Function and Overexpression of the GALS Genes Leads to Altered RG-I Characteristics

Since β -1,4-galactan is found as a backbone decoration in RG-I we further analyzed the RG-I structure of the triple mutant and for comparison material from plants overexpressing *GALS1*. We enriched RG-I from these plants by digesting AIR with a pectin-methylesterase and an endo-polygalacturonase before separation by size-exclusion chromatography and analysis by

HPAEC-PAD. The loss of *GALS* gene function as well as overexpression of the *GALS1* gene resulted in an altered RG-I monosaccharide composition (**Figure 8**), structure (**Table 2**) and concomitantly altered RG-I properties (**Supplementary Figure S6b**). We analyzed the RG-I isolated from the triple mutant and *GALS1* overexpression plants using HPAEC-PAD (**Figure 8**) and glycosidic linkage analysis (**Table 2**). The HPAEC-PAD data showed a RG-I-specific increase in Gal in the overexpression plants and the reduction of Gal in the triple mutant (**Figure 8**). The change in RG-I Gal content in the mutant plants is also evident when the ratio between Gal and the backbone sugar Rha is calculated (**Supplementary Figure S6a**). These modifications, furthermore, affect the degree of polymerization of RG-I since overexpression causes earlier RG-I elution, while RG-I enriched from the triple mutant elutes later than the WT and the 35S-YFP-*GALS1* extracts (**Supplementary Figure S6b**).

To learn more about the RG-I structure in these mutant plants we performed linkage analysis (**Table 2**). This analysis revealed that in RG-I extracts from the triple mutant, the amount of the 1,4-linked Gal was undetectable; whereas in RG-I from the 35S-YFP-*GALS1* this linkage showed a significant increase of 11.5% as compared to 5.5% in the WT. When compared to the WT, other linkages were not substantially affected in the triple mutant and the 35S-YFP-*GALS1* overexpression line consistent with the microarray profiling data. Smaller changes were observed for 1,5-Ara, which was reduced (10.5%) in the overexpression line, but slightly increased in the triple mutant (14.4%) in comparison to the WT (13.3%), suggesting that galactans and arabinans may be competing for sites during RG-I biosynthesis. The same pattern was observed for 1,3-Gal and 1,6-Gal, which were also decreased in the *GALS1* overexpression line and increased in the triple mutant. Notably, the 1,2-Rha and 1,2,4-Rha, representing unbranched and branched Rha, respectively, were unchanged in the mutant plants. This shows that the RG-I in both the triple mutant and the *GALS1* overexpressing line has the same degree of branching and in the triple mutant the branches must consist of single or at most very few Gal residues.

DISCUSSION

Although pectin biosynthesis has been intensively studied for decades, only a few enzymes directly involved in synthesizing pectic polysaccharides have been identified and characterized (Atmodjo et al. 2013). In this study we present unequivocal biochemical and *in planta* evidence that *GALS2* and *GALS3*, in addition to the previously reported *GALS1*, i.e.

all three members of the Arabidopsis GT family 92 are active β -1,4-galactan synthases. All three proteins were able to transfer Gal onto galactopentaose and the activity of GALS1 increased when longer acceptors such as galactohexaose or galactohptaose were provided, which is in agreement with what we have reported using the less quantitative PACE assay (Laursen et al. 2018). In our assay the highest activity was detected when galactohptaose was added to the reaction mix, similarly to what has been reported earlier for β -1,4-galactan synthase activity detected in crude microsomal membrane preparations from mung bean (Ishii et al. 2004) and soybean hypocotyls (Konishi et al. 2007). Since activity of the GALS proteins increased with the length of the acceptor it is likely that the GALS proteins favor acceptors even longer than the galactohptaose, although the activity level was clearly leveling off by DP = 7.

Interestingly, the GALS proteins require linear galacto-oligosaccharides for acceptors since no substantial activity could be observed when multiple branched acceptors with Ara or Gal decorations were tested. This finding suggests that the synthesis of the galactan side chains occurs first and that the galactans are elongated to their full length before other sugar molecules such as Ara or Gal are added.

To investigate the *in vivo* functions of GALS2 and GALS3, we overexpressed the proteins using stable transformations of Arabidopsis. Like GALS1, GALS2 and GALS3 overexpression led to a significant increase in Gal of up to more than 50%. The additional Gal contained in these plants was mainly found to be β -1,4-galactan as had been shown earlier for GALS1. These results demonstrate that the GALS1 homologs GALS2 and GALS3 also function as β -1,4-galactan synthases both *in vitro* and *in vivo*.

The cell wall composition was very similar for all overexpression lines despite the lower activity of GALS2 and GALS3 *in vitro*, suggesting that β -1,4-galactan synthesis *in vivo* became limited by other factors. Most likely, substrate became limited, since we have shown earlier that overexpression of the UDP-Gal/UDP-Rha transporter 1 (URGT1) also results in increased β -1,4-galactan accumulation (Rautengarten et al. 2014).

To probe the functional relation of the three genes in more detail we generated double and triple mutants, and anticipated they would contain less cell wall Gal when compared to the single mutants. In the triple mutant and the *gals2-1/gals3-1* double mutant labeling with the LM5 antibody gave no signal, suggesting that 1,4-linked Gal with more than two contiguous residues was absent. Consistent with this, linkage analysis could not detect 1-4-linked Gal in

the triple mutant. These observations indicated, as predicted by Mohnen (2008), that one or more yet unidentified enzymes are required to attach the first one or few Gal residues onto the RG-I backbone and thereafter the GALS proteins continue the extension of the galactan chains.

Remarkably, even though *GALS* triple mutant plants contain no elongated galactans and concomitantly the structure of RG-I is altered, no morphological changes compared to WT plants were observed. The same lack of an obvious phenotype was observed for plants overexpressing either one of the three GALS proteins, which accumulate significant amounts of additional cell wall-bound Gal as β -1,4-galactan but are morphologically indistinguishable from WT plants. Similarly to our results, potato tubers expressing a fungal endo-galactanase showed a 30% reduction in Gal content but did not display any obvious phenotypical alterations compared to the WT (Oxenboll Sorensen et al. 2000). However, alterations of the biomechanical properties of these potato tubers have been reported (Ulvskov et al. 2005) and therefore it cannot be excluded that mechanical cell wall properties of the *GALS* mutant plants might also be different from those of the WT. Additional experiments assessing the tensile strength of the *GALS* mutant stems will be required to determine whether this is the case. In a different study, Arabidopsis plants expressing an apoplast-targeted galactanase, which led to a substantial reduction in the galactan epitope, bolted later and displayed a reduced stem diameter compared to WT plants (Obro et al. 2009). However, these kinds of morphological and developmental changes were not observed in the *gals1/gals2/gals3* triple mutant, suggesting that those were likely a specific response to the introduction of the fungal galactanase and not the result of changes in RG-I galactan structure. That contrasts with what has been observed for the arabinan sidechains of RG-I, because mutant lines containing ~30% more arabinose in their cell walls showed reduced growth and early senescing leaves (Rautengarten et al. 2017).

Nonetheless, our results indicate a high degree of flexibility for the composition of RG-I, with respect to the length of the β -1,4-galactan side chains.

GALS proteins are highly conserved, and β -1,4-galactan is found throughout the plant kingdom. Therefore, it is likely that β -1,4-galactans have important functions even though they were not apparent in our experiments. We suggest that the biological significance of β -

1,4-galactans may be more apparent under specific stress conditions different from those applied in this study or during specific developmental events.

Galactans are abundant in the G-layer of cell walls in tension wood formed in woody angiosperms (Foston et al. 2011; Mellerowicz and Gorshkova 2012). The presence of high levels of galactan in secondary walls of tension wood has increased the focus on galactan as target to increase the ratio of hexoses to pentoses in plant biomass (Loque et al. 2015) which is a desired trait for the conversion of lignocellulosic biomass into fuels (Vega-Sanchez et al. 2015). As a result, the recent application of stacking strategies targeting genes involved in galactan biosynthesis such as GALS1, URGT1 and UGE2 have led to plant biomass with improved properties for biofuel production (Aznar et al. 2018; Gondolf et al. 2014).

MATERIAL AND METHODS

Plant Material and Plant Growth

Arabidopsis (*Arabidopsis thaliana* (L.) Heynh.) Columbia-0 (Col-0) and T-DNA insertional mutants were obtained from the Arabidopsis Biological Resource Center (ABRC) and the European Arabidopsis Stock Centre (NASC). Detailed information about the T-DNA lines and the GALS1 overexpression line has been reported earlier (Liwanag et al. 2012). For growth in liquid culture, seeds were surface sterilized and grown for 10 to 14 days in 0.5× Murashige and Skoog (MS) basal salt medium (Phyto Technology Laboratories) supplemented with 1% sucrose (Suc) (w/v) and adjusted to pH 5.8 with 1 m KOH at 22°C under constant moderate light and shaking (125 rpm). To test the response to high sucrose, the actin inhibitor Latrunculin B (LatB) and the cellulose inhibitor isoxaben, seeds were surface sterilized and directly germinated on 0.5× MS plates containing either 3.5% Suc, 2 nM isoxaben or 100 nM LatB, respectively. The effects of isoxaben and LatB treatments were studied in dark-grown hypocotyls 7 days after planting the seeds, while high sucrose responses were studied in roots of 7 day-old plants. For salt stress experiments, seeds were grown for 2-3 days on 0.5× MS plates supplemented with 1% Suc before seedlings were transferred to plates containing 130 mM NaCl. Root measurements were undertaken after seedlings were grown for additional five days. The length of hypocotyls and roots was determined using the plant image analysis software WinRHIZO and graphs generated using BoxBlotR (Spitzer et al. 2014). For all other experiments, plants were grown on soil (PRO-

MIX) under short-day light conditions (10 h of fluorescent light [$120 \mu\text{mol m}^{-2} \text{s}^{-1}$]) and 14 h of dark at 22°C, 60% relative humidity (RH). After 4 weeks plants were transferred to long-day conditions (16 h light / 8 h of dark). To identify homozygous lines, PCR was performed using primers described previously (Liwanag et al. 2012).

RNA Isolation and Quantitative RT-PCR Analysis

One leaf was instantly placed in liquid nitrogen and RNA was isolated using the RNeasy RNA Plant Kit (Qiagen) including on-column DNase I digestion removing DNA contaminants. Resultant RNA was quantified and 500 ng were used as template for cDNA synthesis with Superscript II (Invitrogen). Semi-quantitative RT-PCR was performed with cDNA as template and primers spanning the full-length sequence of the transcript (**Supplementary Figure S3**). Quantitative Real-time PCR was essentially performed as described (Ebert et al. 2015) using primers listed in **Supplementary Table S1**. As references, *UBQ10* (At4g05320) *PP2A* (At1g13320) and *MON1* (At2g28390) were employed (**Supplementary Table S1**). The expression levels of each sample were normalized against the geometric average of the three housekeeping genes according to the normalization strategy from (Vandesompele et al. 2002).

Subcellular Localization Analysis of GALS2 and GALS3

Coding sequences for Arabidopsis GALS2 and GALS3 without the native stop codon were PCR amplified from genomic DNA using primers listed in Table S1. To generate the respective entry clones the resultant PCR products were introduced into the pENTR/SD/D-TOPO vector (Thermo Fisher Scientific). C-terminal YFP fusions were created by introduction of the constructs into the pEarleyGate101 plant transformation vector (Earley et al. 2006) using LR Clonase II (Thermo Fisher Scientific). Plasmids were verified by sequencing and transformed into *Agrobacterium* GV3101::pMP90 cells. To analyze the subcellular localization, the proteins were transiently expressed in *Nicotiana benthamiana* and visualized by confocal microscopy as described earlier (Rautengarten et al. 2016).

Analysis of the Cell Wall Monosaccharide Composition

Rosette leaves of six-week-old plants were harvested in liquid nitrogen and alcohol insoluble residues (AIR) were recovered and hydrolyzed before quantification of the monosaccharide

composition by High-Performance Anion-Exchange Chromatography coupled with Pulsed Amperometric Detection (HPAEC-PAD). These steps were performed according to (Rautengarten et al. 2016). In brief, plant material was ground to a fine powder, washed with aqueous ethanol and acetone, hydrolyzed with 2 M trifluoroacetic acid (TFA) for 1 h at 120°C, dried and resuspended in sterile water. The samples were then analyzed on a Dionex ICS3000 instrument using a NaOH gradient. Due to the omission of a de-starching step the glucose (Glc) content was not determined.

Generation and Analysis of 35S-YFP-GALS2 and 35S-YFP-GALS3 Plants

Coding sequences for Arabidopsis *GALS2* and *GALS3* without the native start codon but with the native stop codon were PCR amplified from genomic DNA (primers listed in Table S1). Resultant PCR products were introduced into the pENTR/SD/D-TOPO cloning vector (Thermo Fisher Scientific) and N-terminal YFP fusions were created by introducing the constructs into the pEarleyGate104 plant transformation vector (Earley et al. 2006) using LR Clonase II (Thermo Fisher Scientific). The constructs were transformed into *Agrobacterium* GV3101::pMP90 cells and stably incorporated into Arabidopsis Col-0 employing the floral dip method (Clough and Bent 1998). AIR preparation, TFA hydrolysis and monosaccharide analysis were performed as described above. To determine the 1,4-linked β -galactan content in plants overexpressing the GALS proteins, AIR was digested with an endo- β -1,4-galactanase from *Aspergillus niger* (Megazyme) following the protocol from (Liwanag et al. 2012). Pellet and supernatant were analyzed by HPAEC-PAD.

Protein Expression in *N. benthamiana* and Microsome Preparation

Agrobacterium GV3101::pMP90 cells carrying the YFP fusion construct or the p19 gene from tomato bushy stunt virus were grown overnight, pelleted at 4000g (10 min, 15°C), washed and re-suspended in 10 mM MES, 10 mM MgCl₂, 100 μ M acetosyringone infiltration buffer, yielding a final OD₆₀₀ value of 0.15. Leaves of four-week-old *N. benthamiana* plants grown in 16/8 h light/dark, 25/24°C and 60% relative humidity were co-infiltrated with the two *Agrobacterium* mixtures using a 1 ml syringe. After two additional days of growth, protein expression was verified by monitoring YFP fluorescence with an epifluorescence microscope. Three days after infiltration, five leaves were harvested and microsomes were extracted as detailed in (Rennie et al. 2012).

Protein Extraction and Immunoblotting

Protein extraction from *N. benthamiana* leaves transiently overexpressing the GALS proteins (35S-FLAG-GALS) and immunoblotting were performed as previously described (Rennie et al. 2012). In brief, at 4°C microsomal proteins were solubilized by incubating with 1% Triton X-100 for 10 min and afterwards centrifuging at 100,000g for 30 min. Subsequently, the resultant supernatant was incubated for 3 h with EZview Red anti-HA resin (Sigma-Aldrich), washed three times with a buffer containing 1% Triton X-100, 400 mM Suc, 50 mM HEPES-KOH, pH 7.0, and 200 mM NaCl. Following that three additional washing steps with 400 mM Suc and 50 mM HEPES-KOH, pH 7.0 were performed. Resin-bound protein was used directly in the GalT assays. For immunoblot analysis, proteins were resolved by SDS-PAGE on 8% to 16% gradient gels (Bio-Rad Mini PROTEAN TGX) and blotted onto nitrocellulose membranes (GE Healthcare). Blots were probed with a 1:10,000 dilution of mouse anti-FLAG antibody (Sigma-Aldrich), followed by a 1:10,000 dilution of goat anti-mouse IgG conjugated to horseradish peroxidase (Sigma-Aldrich), before applying ECL detection reagent (SuperSignal West Extended Duration Substrate). Imaging of the blots was done with the Amersham Imager 600 (GE Healthcare).

Galactosyltransferase Assays

The GalT activity using microsomal preparations was determined as previously described (Liwanag et al. 2012) using 40 µg microsomal protein, 10 nCi UDP-[¹⁴C]Gal, and 20 mM of the respective acceptor per 50 µl reaction. For reactions with purified GALS1, GALS2 and GALS3, an amount of protein corresponding to 100 mg of microsomal protein was used in each assay performed as described (Liwanag et al. 2012). Linear and branched galactan substrates were prepared by coupling of protected mono- and disaccharide building blocks followed by global deprotection and purification by chromatography on C18-modified silica (Andersen et al. 2016b).

ANTS Labeling and Analysis of Labeled Galactan Substrates

Galactan substrates (200 µg of each oligosaccharide) were reductively aminated with 8-aminonaphthalene-1,3,6-trisulfonic acid (ANTS) as follows: to each tube were added 5 µl of 0.2 M ANTS solution (resuspended in 17:3, water:acetic acid) and 5 µl of 0.2 M 2-picoline

borane (resuspended in DMSO) as described earlier (Mortimer et al. 2015). Samples were dried and resuspended in 100 µl sterile water. Excess fluorophore was removed using GlykoClean S Cartridges (Prozyme). Labeled oligosaccharides were dried and resuspended to a concentration of 1 µg/µl.

Polysaccharide Analysis by Carbohydrate Gel Electrophoresis (PACE)

All reactions were performed in a total volume of 25 µl containing MnCl₂ (10 mM), Triton X-100 (1% v/v) in buffer (50 mM MES, pH 6.5) with different Gal_n substrates (2 µg), UDP-galactose (200 µM) and microsomal membranes. Reactions were incubated for 2 h at 30°C under shaking. Reactions were terminated by heating (100°C, 3 min) and precipitated protein and lipids were collected by centrifugation (10,000 g for 10 min). Supernatants (15 µl) were mixed with 15 µl urea (3 M), subsequently the samples (5 µl) were analyzed on large format Tris-borate acrylamide gels prepared as described elsewhere (Goubet et al. 2002) and separated at 200V for 30 min followed by 1000V for 1.5 h. PACE gels were visualized with a G-box (Syngene) equipped with UV detection filter and long-wave UV tubes (365 nm emission).

Enrichment and Analysis of Rhamnogalacturonan-I (RG-I)

RG-I was enriched from pooled leaf material of six-week-old plants as described previously (Stonebloom et al. 2016). In brief, AIR was solubilized in 50 mM ammonium oxalate (pH 5.0) and digested overnight with pectin methyl-esterase (Novozymes) and polygalacturonanase (Megazyme) at 37°C. After the digestion step, insoluble material was removed by centrifugation and filtration using a 0.45 µm spin filter. Oligosaccharides and residual digestion buffer were removed by repeating washing steps of the solubilized polysaccharides on a 10 kDa Cutoff spin filter (Amicon) with sterile water. Samples were eluted in water and separated by size-exclusion chromatography in 50 mM ammonium formate (pH 5.0) on a Superdex 200 10/300GL column (GE Healthcare). Elution of polysaccharides was monitored with a RI-101 refractive index detector (Shodex), fractions were manually collected, lyophilized, TFA hydrolyzed and subsequently analyzed by HPAEC-PAD. Dextran molecular weight standards (Sigma-Aldrich) were used to estimate the molecular weight of RG-I.

Immunodot Blot Analysis

AIR (5-15 mg) from whole rosettes (or as control potato galactan and sugar beet pectin) were washed with liquefied phenol:acetic acid:water (2:1:1) for 3.5 h at room temperature. Subsequently, samples were pelleted, washed three times with water and dried in a vacuum concentrator. The samples were extracted by ball milling in 4 M KOH with 0.1% NaBH₄. After a centrifugation step the supernatant was transferred into a new tube and neutralized with HCl. The samples were diluted and 1 µl of each of the dilutions was spotted onto a nitrocellulose membrane. Dry membranes were washed with 1xPBS, and blocked with 1xPBS containing 5% non-fat milk. Blots were probed with a 1:300 dilution of the primary antibody, followed by a 1:5,000 dilution of goat anti-mouse IgG conjugated to horseradish peroxidase (Sigma-Aldrich), before applying ECL detection reagent (SuperSignal West Extended Duration Substrate). Imaging of the blots was done with the Amersham Imager 600 (GE Healthcare).

Microarray Polymer Profiling

Microarray polymer profiling was undertaken essentially following the protocol previously published (Moller et al. 2007). AIR was prepared from mutant and WT plants grown in liquid culture. AIR (10 mg) was sequentially extracted with 50 mM CDTA and 1 M NaOH to obtain pectin-rich and hemicellulose-rich extracts respectively. The experiment was performed in triplicates. The resultant cell wall extracts were spotted onto membranes and subsequently probed with monoclonal antibodies and carbohydrate-binding modules that recognize specific cell wall epitopes namely JIM5, JIM7, JIM13, LM5, LM6, LM11, LM18, LM19, LM25, INRA-RU1, INRA-RU2, AX1 and CBM3A (Blake et al. 2006; Clausen et al. 2003; Guillon et al. 2004; Jones et al. 1997; Knox et al. 1991; McCartney et al. 2005; Pedersen et al. 2012; Ralet et al. 2010; Verhertbruggen et al. 2009; Willats et al. 1998).

Glycosidic Linkage Analysis of Rhamnogalacturonan-I

Glycosidic linkage analysis was performed with minor modifications as described by (Pettolino et al. 2012). RG-I enriched samples underwent carboxyl reduction (Kim and Carpita 1992). Samples were sequentially reduced with 3x1 ml of 100 mg/ml NaBD₄ in 1 M imidazole, neutralized with 500 µl glacial acetic acid, dialyzed overnight in 6000-8000 Da molecular weight cut-off dialysis tubing, re-dissolved in 0.2 M MES and 400 µl of 500

mg/ml carbodiimide reagent, split and further reduced with 1 ml of 70 mg/ml NaBH₄ or NaBD₄ in 4 M imidazole, neutralized with 500 µl glacial acetic acid, dialyzed again overnight and freeze dried. Samples were re-dissolved in 100 µl DMSO and per-*O*-methylated using 100 µl of 120 mg/ml NaOH/DMSO slurry, sonicated for 20 min and further sonicated for 10/10/20 min after the addition of 20/20/40 µl of methyl iodide, respectively, before being washed three times in a 3:1 mix of water:dichloromethane before being dried under nitrogen. They were further derivatized to their corresponding partially methylated alditol acetates by hydrolysis for 1.5 h at 121°C with 100 µl of 2 M trifluoroacetic acid and dried under nitrogen. Reduction was achieved by dissolving in 50 µl of 2 M NH₄OH, adding 50 µl of 1 M NaBD₄ in 2 M NH₄OH and incubated at room temperature for 2.5 h before being neutralized with 20 µl glacial acetic acid, washed sequentially whilst under a stream of nitrogen with 2x 250 µl 5% acetic acid in methanol and 3x 250 µl methanol and dried under nitrogen. Samples were per-*O*-acetylated by incubating at 100°C with 250 µl acetic anhydride before neutralization with 3 ml of water, then washed in a biphasic 3:1 mix of water:dichloromethane. The non-polar phase was dried under nitrogen and reconstituted in 100 µl dichloromethane and separated using a gas chromatograph (Agilent 7890A) equipped with a BPX70 GC capillary column (SGE Analytical Science) and a mass spectrometer (Agilent 5975C) using a temperature gradient. Eluted compounds were identified based on their retention time compared to standards and their ion fragmentation patterns.

Accession Numbers

Sequence data used in this study was retrieved from The Arabidopsis Information Resource (TAIR): AT2G33570 (*GALS1*), AT5G44670 (*GALS2*), AT4G20170 (*GALS3*), At1g13320 (*PP2A*), At2g28390 (*MON1*), At4g05320 (*UBI10*), and AT3G18780 (*ACTIN2*).

SUPPLEMENTARY DATA

Supplementary data are available at PCP online

FUNDING

This work was supported by the U. S. Department of Energy, Office of Science, Office of Biological and Environmental Research, through contract DE-AC02-05CH11231 between

Lawrence Berkeley National Laboratory and the U. S. Department of Energy, the Danish Strategic Research Council [Set4Future 11-116795] to H.V.S., Australian Research Council [FT160100276, FT130101165] to B.E. and J.L.H., the Villum Foundation (PLANET project) and the Novo Nordisk Foundation (Biotechnology-based Synthesis and Production Research) to M.C.F.A., M.H.C., the Villum Foundation (95-300-73023) to T.L., the ARC Centre of Excellence in Plant Cell Walls [CE110001007] to A.B.

DISCLOSURES

The authors have no conflict of interest to declare.

REFERENCES

- Andersen, M.C., Boos, I., Marcus, S.E., Kracun, S.K., Rydahl, M.G., Willats, W.G., et al. (2016a) Characterization of the LM5 pectic galactan epitope with synthetic analogues of beta-1,4-d-galactotetraose. *Carbohydrate research* 436: 36-40.
- Andersen, M.C., Kracun, S.K., Rydahl, M.G., Willats, W.G. and Clausen, M.H. (2016b) Synthesis of beta-1,4-Linked Galactan Side-Chains of Rhamnogalacturonan I. *Chemistry* 22: 11543-11548.
- Arend, M. (2008) Immunolocalization of (1,4)-beta-galactan in tension wood fibers of poplar. *Tree Physiol* 28: 1263-1267.
- Arsovski, A.A., Haughn, G.W. and Western, T.L. (2010) Seed coat mucilage cells of *Arabidopsis thaliana* as a model for plant cell wall research. *Plant signaling & behavior* 5: 796-801.
- Atmodjo, M.A., Hao, Z.Y. and Mohnen, D. (2013) Evolving Views of Pectin Biosynthesis. *Annu Rev Plant Biol* 64: 747-+.
- Atmodjo, M.A., Sakuragi, Y., Zhu, X., Burrell, A.J., Mohanty, S.S., Atwood, J.A., 3rd, et al. (2011) Galacturonosyltransferase (GAUT)1 and GAUT7 are the core of a plant cell wall pectin biosynthetic homogalacturonan:galacturonosyltransferase complex. *Proc Natl Acad Sci U S A* 108: 20225-20230.

- Aznar, A., Chalvin, C., Shih, P.M., Maimann, M., Ebert, B., Birdseye, D.S., et al. (2018) Gene stacking of multiple traits for high yield of fermentable sugars in plant biomass. *Biotechnology for biofuels* 11: 2.
- Bidhendi, A.J. and Geitmann, A. (2016) Relating the mechanics of the primary plant cell wall to morphogenesis. *J Exp Bot* 67: 449-461.
- Blake, A.W., McCartney, L., Flint, J.E., Bolam, D.N., Boraston, A.B., Gilbert, H.J., et al. (2006) Understanding the biological rationale for the diversity of cellulose-directed carbohydrate-binding modules in prokaryotic enzymes. *The Journal of biological chemistry* 281: 29321-29329.
- Blamey, F.P.C. (2003) A role for pectin in the control of cell expansion. *Soil Sci Plant Nutr* 49: 775-783.
- Clausen, M.H., Willats, W.G. and Knox, J.P. (2003) Synthetic methyl hexagalacturonate hapten inhibitors of anti-homogalacturonan monoclonal antibodies LM7, JIM5 and JIM7. *Carbohydrate research* 338: 1797-1800.
- Clough, S.J. and Bent, A.F. (1998) Floral dip: a simplified method for *Agrobacterium*-mediated transformation of *Arabidopsis thaliana*. *Plant J* 16: 735-743.
- Daher, F.B. and Braybrook, S.A. (2015) How to let go: pectin and plant cell adhesion. *Front Plant Sci* 6: 523.
- de Vries, R.P. and Visser, J. (2001) *Aspergillus* enzymes involved in degradation of plant cell wall polysaccharides. *Microbiol Mol Biol Rev* 65: 497-522, table of contents.
- Driouich, A., Follet-Gueye, M.L., Bernard, S., Kousar, S., Chevalier, L., Vire-Gibouin, M., et al. (2012) Golgi-mediated synthesis and secretion of matrix polysaccharides of the primary cell wall of higher plants. *Front Plant Sci* 3: 79.
- Du, S. and Yamamoto, F. (2007) An overview of the biology of reaction wood formation. *J Integr Plant Biol* 49: 131-143.

- Dumont, M., Lehner, A., Bouton, S., Kiefer-Meyer, M.C., Voxeur, A., Pelloux, J., et al. (2014) The cell wall pectic polymer rhamnogalacturonan-II is required for proper pollen tube elongation: implications of a putative sialyltransferase-like protein. *Ann Bot* 114: 1177-1188.
- Earley, K.W., Haag, J.R., Pontes, O., Opper, K., Juehne, T., Song, K., et al. (2006) Gateway-compatible vectors for plant functional genomics and proteomics. *Plant J* 45: 616-629.
- Ebert, B., Rautengarten, C., Guo, X., Xiong, G., Stonebloom, S., Smith-Moritz, A.M., et al. (2015) Identification and Characterization of a Golgi-Localized UDP-Xylose Transporter Family from Arabidopsis. *Plant Cell* 27: 1218-1227.
- Egelund, J., Damager, I., Faber, K., Olsen, C.E., Ulvskov, P. and Petersen, B.L. (2008) Functional characterisation of a putative rhamnogalacturonan II specific xylosyltransferase. *Febs Lett* 582: 3217-3222.
- Egelund, J., Petersen, B.L., Motawia, M.S., Damager, I., Faik, A., Olsen, C.E., et al. (2006) Arabidopsis thaliana RGXT1 and RGXT2 encode Golgi-localized (1,3)-alpha-D-xylosyltransferases involved in the synthesis of pectic rhamnogalacturonan-II. *Plant Cell* 18: 2593-2607.
- Foston, M., Hubbell, C.A., Samuel, R., Jung, S., Fan, H., Ding, S.Y., et al. (2011) Chemical, ultrastructural and supramolecular analysis of tension wood in *Populus tremula x alba* as a model substrate for reduced recalcitrance. *Energ Environ Sci* 4: 4962-4971.
- Gondolf, V.M., Stoppel, R., Ebert, B., Rautengarten, C., Liwanag, A.J., Loque, D., et al. (2014) A gene stacking approach leads to engineered plants with highly increased galactan levels in Arabidopsis. *BMC plant biology* 14: 344.
- Gorshkova, T., Mokshina, N., Chernova, T., Ibragimova, N., Salnikov, V., Mikshina, P., et al. (2015) Aspen Tension Wood Fibers Contain beta-(1---> 4)-Galactans and Acidic Arabinogalactans Retained by Cellulose Microfibrils in Gelatinous Walls. *Plant Physiol* 169: 2048-2063.
- Gorshkova, T. and Morvan, C. (2006) Secondary cell-wall assembly in flax phloem fibres: role of galactans. *Planta* 223: 149-158.

- Goubet, F., Jackson, P., Deery, M.J. and Dupree, P. (2002) Polysaccharide analysis using carbohydrate gel electrophoresis: a method to study plant cell wall polysaccharides and polysaccharide hydrolases. *Analytical biochemistry* 300: 53-68.
- Guillon, F., Tranquet, O., Quillien, L., Utille, J.P., Ortiz, J.J.O. and Saulnier, L. (2004) Generation of polyclonal and monoclonal antibodies against arabinoxylans and their use for immunocytochemical location of arabinoxylans in cell walls of endosperm of wheat. *J Cereal Sci* 40: 167-182.
- Hansen, S.F., Harholt, J., Oikawa, A. and Scheller, H.V. (2012) Plant Glycosyltransferases Beyond CAZY: A Perspective on DUF Families. *Front Plant Sci* 3: 59.
- Harholt, J., Jensen, J.K., Sorensen, S.O., Orfila, C., Pauly, M. and Scheller, H.V. (2006) ARABINAN DEFICIENT 1 is a putative arabinosyltransferase involved in biosynthesis of pectic arabinan in Arabidopsis. *Plant Physiol* 140: 49-58.
- Harholt, J., Jensen, J.K., Verhertbruggen, Y., Sogaard, C., Bernard, S., Nafisi, M., et al. (2012) ARAD proteins associated with pectic Arabinan biosynthesis form complexes when transiently overexpressed in planta. *Planta* 236: 115-128.
- Harholt, J., Suttangkakul, A. and Vibe Scheller, H. (2010) Biosynthesis of pectin. *Plant Physiol* 153: 384-395.
- Ishii, T., Ohnishi-Kameyama, M. and Ono, H. (2004) Identification of elongating beta-1,4-galactosyltransferase activity in mung bean (*Vigna radiata*) hypocotyls using 2-aminobenzaminated 1,4-linked beta- D-galactooligosaccharides as acceptor substrates. *Planta* 219: 310-318.
- Jensen, J.K., Sorensen, S.O., Harholt, J., Geshi, N., Sakuragi, Y., Moller, I., et al. (2008) Identification of a xylogalacturonan xylosyltransferase involved in pectin biosynthesis in Arabidopsis. *Plant Cell* 20: 1289-1302.
- Jones, L., Seymour, G.B. and Knox, J.P. (1997) Localization of Pectic Galactan in Tomato Cell Walls Using a Monoclonal Antibody Specific to (1[->]4)-[beta]-D-Galactan. *Plant Physiol* 113: 1405-1412.

Kim, J.B. and Carpita, N.C. (1992) Changes in Esterification of the Uronic Acid Groups of Cell Wall Polysaccharides during Elongation of Maize Coleoptiles. *Plant Physiol* 98: 646-653.

Knox, J.P., Linstead, P.J., Cooper, J.P.C. and Roberts, K. (1991) Developmentally regulated epitopes of cell surface arabinogalactan proteins and their relation to root tissue pattern formation. *Plant J* 1: 317-326.

Konishi, T., Kotake, T. and Tsumuraya, Y. (2007) Chain elongation of pectic beta-(1-->4)-galactan by a partially purified galactosyltransferase from soybean (*Glycine max* Merr.) hypocotyls. *Planta* 226: 571-579.

Laursen, T., Stonebloom, S.H., Pidatala, V.R., Birdseye, D.S., Clausen, M.H., Mortimer, J.C., et al. (2018) Bifunctional glycosyltransferases catalyze both extension and termination of pectic galactan oligosaccharides. *Plant J* 94: 340-351.

Liu, X.L., Liu, L., Niu, Q.K., Xia, C., Yang, K.Z., Li, R., et al. (2011) Male gametophyte defective 4 encodes a rhamnogalacturonan II xylosyltransferase and is important for growth of pollen tubes and roots in *Arabidopsis*. *Plant J* 65: 647-660.

Liwanag, A.J., Ebert, B., Verhertbruggen, Y., Rennie, E.A., Rautengarten, C., Oikawa, A., et al. (2012) Pectin biosynthesis: GAL51 in *Arabidopsis thaliana* is a beta-1,4-galactan beta-1,4-galactosyltransferase. *The Plant cell* 24: 5024-5036.

Loque, D., Scheller, H.V. and Pauly, M. (2015) Engineering of plant cell walls for enhanced biofuel production. *Curr Opin Plant Biol* 25: 151-161.

Mast, S.W., Donaldson, L., Torr, K., Phillips, L., Flint, H., West, M., et al. (2009) Exploring the ultrastructural localization and biosynthesis of beta(1,4)-galactan in *Pinus radiata* compression wood. *Plant Physiol* 150: 573-583.

McCartney, L., Marcus, S.E. and Knox, J.P. (2005) Monoclonal antibodies to plant cell wall xylans and arabinoxylans. *The journal of histochemistry and cytochemistry : official journal of the Histochemistry Society* 53: 543-546.

- McNab, J.M., Villemez, C.L. and Albersheim, P. (1968) Biosynthesis of galactan by a particulate enzyme preparation from *Phaseolus aureus* seedlings. *Biochem J* 106: 355-360.
- Mellerowicz, E.J. and Gorshkova, T.A. (2012) Tensional stress generation in gelatinous fibres: a review and possible mechanism based on cell-wall structure and composition. *Journal of experimental botany* 63: 551-565.
- Mohnen, D. (2008) Pectin structure and biosynthesis. *Curr Opin Plant Biol* 11: 266-277.
- Moller, I., Sorensen, I., Bernal, A.J., Blaukopf, C., Lee, K., Obro, J., et al. (2007) High-throughput mapping of cell-wall polymers within and between plants using novel microarrays. *Plant J* 50: 1118-1128.
- Mortimer, J.C., Faria-Blanc, N., Yu, X., Tryfona, T., Sorieul, M., Ng, Y.Z., et al. (2015) An unusual xylan in *Arabidopsis* primary cell walls is synthesised by GUX3, IRX9L, IRX10L and IRX14. *Plant J* 83: 413-426.
- Ndeh, D., Rogowski, A., Cartmell, A., Luis, A.S., Basle, A., Gray, J., et al. (2017) Complex pectin metabolism by gut bacteria reveals novel catalytic functions. *Nature* 544: 65-70.
- Nelson, B.K., Cai, X. and Nebenfuhr, A. (2007) A multicolored set of in vivo organelle markers for co-localization studies in *Arabidopsis* and other plants. *Plant J* 51: 1126-1136.
- Obro, J., Borkhardt, B., Harholt, J., Skjot, M., Willats, W.G. and Ulvskov, P. (2009) Simultaneous in vivo truncation of pectic side chains. *Transgenic Res* 18: 961-969.
- Oxenboll Sorensen, S., Pauly, M., Bush, M., Skjot, M., McCann, M.C., Borkhardt, B., et al. (2000) Pectin engineering: modification of potato pectin by in vivo expression of an endo-1,4-beta-D-galactanase. *Proc Natl Acad Sci U S A* 97: 7639-7644.
- Pedersen, H.L., Fangel, J.U., McCleary, B., Ruzanski, C., Rydahl, M.G., Ralet, M.C., et al. (2012) Versatile high resolution oligosaccharide microarrays for plant glycobiology and cell wall research. *The Journal of biological chemistry* 287: 39429-39438.
- Pettolino, F.A., Walsh, C., Fincher, G.B. and Bacic, A. (2012) Determining the polysaccharide composition of plant cell walls. *Nature protocols* 7: 1590-1607.

- Qu, F. and Morris, T.J. (2002) Efficient infection of *Nicotiana benthamiana* by Tomato bushy stunt virus is facilitated by the coat protein and maintained by p19 through suppression of gene silencing. *Molecular plant-microbe interactions* : MPMI 15: 193-202.
- Ralet, M.C., Tranquet, O., Poulain, D., Moise, A. and Guillon, F. (2010) Monoclonal antibodies to rhamnogalacturonan I backbone. *Planta* 231: 1373-1383.
- Rasul, S., Dubreuil-Maurizi, C., Lamotte, O., Koen, E., Poinssot, B., Alcaraz, G., et al. (2012) Nitric oxide production mediates oligogalacturonide-triggered immunity and resistance to *Botrytis cinerea* in *Arabidopsis thaliana*. *Plant Cell Environ* 35: 1483-1499.
- Rautengarten, C., Birdseye, D., Pattathil, S., McFarlane, H.E., Saez-Aguayo, S., Orellana, A., et al. (2017) The elaborate route for UDP-arabinose delivery into the Golgi of plants. *Proc Natl Acad Sci U S A* 114: 4261-4266.
- Rautengarten, C., Ebert, B., Liu, L.F., Stonebloom, S., Smith-Moritz, A.M., Pauly, M., et al. (2016) The *Arabidopsis* Golgi-localized GDP-L-fucose transporter is required for plant development. *Nature Communications* 7: 12119.
- Rautengarten, C., Ebert, B., Moreno, I., Temple, H., Herter, T., Link, B., et al. (2014) The Golgi localized bifunctional UDP-rhamnose/UDP-galactose transporter family of *Arabidopsis*. *Proc Natl Acad Sci U S A* 111: 11563-11568.
- Rennie, E.A., Hansen, S.F., Baidoo, E.E., Hadi, M.Z., Keasling, J.D. and Scheller, H.V. (2012) Three members of the *Arabidopsis* glycosyltransferase family 8 are xylan glucuronosyltransferases. *Plant Physiol* 159: 1408-1417.
- Ridley, B.L., O'Neill, M.A. and Mohnen, D.A. (2001) Pectins: structure, biosynthesis, and oligogalacturonide-related signaling. *Phytochemistry* 57: 929-967.
- Spitzer, M., Wildenhain, J., Rappsilber, J. and Tyers, M. (2014) BoxPlotR: a web tool for generation of box plots. *Nature Methods* 11: 121-122.
- Sterling, J.D., Atmodjo, M.A., Inwood, S.E., Kumar Kolli, V.S., Quigley, H.F., Hahn, M.G., et al. (2006) Functional identification of an *Arabidopsis* pectin biosynthetic homogalacturonan galacturonosyltransferase. *Proc Natl Acad Sci U S A* 103: 5236-5241.

Stonebloom, S., Ebert, B., Xiong, G., Pattathil, S., Birdseye, D., Lao, J., et al. (2016) A DUF-246 family glycosyltransferase-like gene affects male fertility and the biosynthesis of pectic arabinogalactans. *Bmc Plant Biol* 16: 90.

Titz, A., Butschi, A., Henrissat, B., Fan, Y.Y., Hennet, T., Razzazi-Fazeli, E., et al. (2009) Molecular basis for galactosylation of core fucose residues in invertebrates: identification of *caenorhabditis elegans* N-glycan core alpha1,6-fucoside beta1,4-galactosyltransferase GALT-1 as a member of a novel glycosyltransferase family. *The Journal of biological chemistry* 284: 36223-36233.

Ulvskov, P., Wium, H., Bruce, D., Jorgensen, B., Qvist, K.B., Skjot, M., et al. (2005) Biophysical consequences of remodeling the neutral side chains of rhamnogalacturonan I in tubers of transgenic potatoes. *Planta* 220: 609-620.

Vandesompele, J., De Preter, K., Pattyn, F., Poppe, B., Van Roy, N., De Paepe, A., et al. (2002) Accurate normalization of real-time quantitative RT-PCR data by geometric averaging of multiple internal control genes. *Genome biology* 3: RESEARCH0034.

Vega-Sanchez, M.E., Loque, D., Lao, J., Catena, M., Verhertbruggen, Y., Herter, T., et al. (2015) Engineering temporal accumulation of a low recalcitrance polysaccharide leads to increased C6 sugar content in plant cell walls. *Plant biotechnology journal* 13: 903-914.

Verhertbruggen, Y., Marcus, S.E., Haeger, A., Ordaz-Ortiz, J.J. and Knox, J.P. (2009) An extended set of monoclonal antibodies to pectic homogalacturonan. *Carbohydrate research* 344: 1858-1862.

Willats, W.G., Marcus, S.E. and Knox, J.P. (1998) Generation of monoclonal antibody specific to (1->5)-alpha-L-arabinan. *Carbohydrate research* 308: 149-152.

TABLE 1. Monosaccharide composition of cell wall preparations recovered from leaves of galactan synthase mutants compared to the WT Col-0 determined by High Performance Anion Exchange Chromatography coupled with Pulsed Amperometric Detection (HPAEC-PAD). WT, wild type. Fuc, fucose. Rha, rhamnose. Ara, arabinose. Gal, galactose. Xyl, xylose, GalA, galacturonic acid. GlcA, glucuronic acid. Values were calculated as mole percent (mol%) of total cell wall sugars and are mean \pm STD; $n = 7$. Student's t -test was performed to determine if mutant lines are statistically different from WT plants and lines showing a significant difference with $P < 0.05$ are indicated in bold.

Plant line	Fuc		Rha		Ara		Gal		Xyl		GalA		GlcA	
	mol%	SD	mol%	SD	mol%	SD	mol%	SD	mol%	SD	mol%	SD	mol%	SD
WT	1.41	0.06	6.48	0.38	16.81	1.89	19.32	0.92	14.53	0.71	39.28	2.90	2.17	0.14
<i>gals1-1</i>	1.67	0.42	7.62	1.80	17.39	2.29	16.07	1.46	15.14	2.06	39.50	4.74	2.61	0.52
<i>gals2-1</i>	1.39	0.15	6.62	0.97	15.59	1.36	18.62	1.14	14.19	1.41	40.95	2.85	2.64	0.76
<i>gals3-1</i>	1.60	0.13	7.58	0.57	16.53	1.46	17.97	1.19	14.52	1.66	39.10	3.31	2.70	0.72
<i>gals1-1/gals3-1</i>	1.64	0.12	7.36	0.75	19.20	1.60	15.30	0.89	16.00	1.15	38.30	2.65	2.21	0.49
<i>gals2-1/gals3-1</i>	1.66	0.12	7.07	1.13	18.85	1.43	15.96	1.40	15.95	1.39	37.71	3.23	2.26	0.56
<i>gals1-1/gals2-1</i>	1.56	0.21	7.16	0.52	16.13	1.47	15.13	0.56	14.70	1.60	42.37	2.84	2.95	0.31
<i>gals1-1/gals2-1/gals3-1</i>	1.60	0.27	8.36	1.94	15.96	1.19	14.53	0.90	14.19	1.52	42.11	4.99	3.25	0.80
35S-YFP-GALS1	1.31	0.10	6.23	0.55	15.87	1.38	27.37	3.07	12.20	0.96	34.54	3.50	2.48	0.71

TABLE 2. Linkage analysis of rhamnogalacturonan-I (RG-I) isolated from the *gals1/gals2/gals3* triple mutant, GALS1 overexpression plants and WT. Rha, rhamnose. Ara, arabinose. Fuc, fucose. Xyl, xylose. Glc, glucose. Gal, galactose. GlcA, glucuronic acid. GalA, galacturonic acid. The values shown are mol%. Linkage analysis was performed with pooled material from two individual RG-I preparations from each genotype.

Derivative	Col-0	35S-YFP-	
Linkage	wild type	GALS1	<i>gals1/gals2/gals3</i>
1,2-Rha (p)	7.3	7.7	8.2
1,2,4-Rha (p)	5.3	5.5	5.7
t-Ara (f)	12.8	12.5	12.1
1,2-Ara (f)	1.9	1.8	1.9
1,5-Ara (f)	13.3	10.5	14.4
1,2,5-Ara (f)	2.2	2.2	2.4
1,3-Fuc (p)	0.9	0.7	0.8
t-Xyl (p)	1.8	1.2	1.8
1,4-Xyl (p)	0.8	0.9	1.0
1,4-Glc (p)	5.6	5.4	3.4
1,4,6-Glc (p)	0.4	0.5	0.3
t-Gal (p)	7.3	6.5	6.1
1,3-Gal (p)	2.9	2.3	3.2
1,4-Gal (p)	5.5	11.5	0.0
1,6-Gal (p)	5.0	4.1	5.7
1,3,4-Gal (p)	1.2	1.4	0.0
1,3,6-Gal (p)	10.4	8.4	10.2
t-GlcA (p)	4.2	3.8	4.7
t-GalA (p)	0.0	1.6	1.5
1,4-GalA (p)	11.1	11.5	15.5
3,4-GalA (p)	0.0	0.0	1.2

FIGURE LEGENDS

FIGURE 1 Sub-cellular localization of the GALS2 and GALS3 proteins. The coding sequences of the proteins were fused to YFP at their C-termini (first row) and compared to the Golgi marker α -mannosidase-I fused to mCherry (middle row). The merged signals (last row) confirm that both GALS2 and GALS3 co-localize with the Golgi marker. Scale bars are 25 μ m.

FIGURE 2 Enzymatic characteristics of the recombinant and affinity-purified YFP-GALS1 protein. (a) pH optimum (b) divalent cations. The data shows averages \pm SEM ($n = 2$).

FIGURE 3 Activity of recombinant purified GALS1 protein probed with various acceptors. **(A)** Structures of galacto-oligosaccharides prepared by chemical synthesis. Galacto-oligosaccharides (compound) 2 to 7 are linear β -1,4-linked structures ranging from with galactobiose (compound 2) to galactoheptaose (compound 7). The remaining structures have a β -1,4-linked hexasaccharide backbone branched at the C6 position of the 4th Gal residue from the reducing end. Compounds 8 to 10 have Gal branches of DP=1 and 2, respectively, whereas 11 and 12 carry α -L-Ara branches of DP=1 and 2, respectively. **(B)** Galactan synthase (GalT) activity of recombinant and purified GALS1 protein transiently overexpressed in *N. benthamiana*. The GalT activity assays were performed with purified 35S-FLAG-GALS1 protein, UDP-[¹⁴C]Gal and different exogenous unbranched acceptors and branched acceptors. Error bars are SEM ($n = 3$ biological replicates). Significant differences from control are indicated (t-test; *, $p < 0.05$; **, $p < 0.01$).

FIGURE 4 Galactan synthase activity of microsomal proteins from *N. benthamiana* overexpressing GALS1, GALS2 and GALS3. **(A)** [¹⁴C]Gal incorporation by microsomal membrane preparations without addition of exogenous acceptor. Plants infiltrated with *A. tumefaciens* containing 35S-FLAG-GALS constructs for GALS1, GALS and GALS3 respectively and p19 and plants infiltrated only with p19 were used as control. Error bars are SEM with $n = 3$ biological replicates. Significant differences from control are indicated (t-test; *, $p < 0.05$; **, $p < 0.01$). **(B)** Immunoblot analysis to assess GALS1, GALS2 and GALS3 protein abundance in the microsomal preparations used in **(A)**.

FIGURE 5 Fluorescent assay determining the activity of recombinant GALS proteins. **(A)** Schematic showing the chemically synthesized galacto-oligosaccharide acceptor reductively coupled with an ANTS fluorescent probe and addition of a Gal moiety from the UDP-Gal precursor onto the growing galacto-oligosaccharide chain as mediated by galactan synthases. **(B)** Immunoblot analysis to assess GALS1, GALS2 and GALS3 protein abundance in microsomal preparations from Arabidopsis plants expressing the three GALS proteins under the CaMV35S promoter. **(c)**, GalT activity of the GALS proteins determined by carbohydrate gel electrophoresis (PACE) using galactopentaose-ANTS as acceptor and UDP-Gal as donor. Protein content was normalized to total microsomal protein or based on protein abundance as determined by immunoblotting.

FIGURE 6 Immunodot blot assays of cell wall extracts isolated from Arabidopsis rosette leaves from mutant and WT plants. The extracts were probed with LM5 for **(A)** 1,4-galactan and **(B)** LM19 for homogalacturonan. **(c)** Microarray polymer profiling analysis with relative abundance of cell wall glycan epitopes in CDTA and NaOH-extracted fractions from alcohol insoluble residue (AIR). Mean and SD for spot signals (MSS) were obtained by probing microarrays with various antibodies recognizing the epitope of representative cell wall polymers (x axis) from four technical replicates with pooled material from eight plants. The highest MSS was set to 100 and all other values adjusted accordingly. Values significantly different from the WT are marked with asterisks (t-test; *, $P < 0.05$; **, $P < 0.01$).

FIGURE 7 Analysis of the monosaccharide composition of leaves from six-week old plants overexpressing *GALS1*, *GALS2* and *GALS3* under the control of the CaMV 35S promoter in comparison to the WT. **(A)** Monosaccharide composition measured by HPAEC-PAD. Values are the mean of eight biological replicates \pm SD. **(B)** Galactose content of cell wall material derived from six-week old WT plants and plants overexpressing the GALS proteins after digestion with endo- β -1,4-galactanase. The supernatant was separated from the insoluble material (residue) and the amount of galactose was measured by HPAEC-PAD. Values are the mean of four replicates \pm SD. Values significantly different from the WT are marked with asterisks (t-test; *, $P < 0.05$; **, $P < 0.01$).

FIGURE 8 Analysis of the monosaccharide composition of rhamnogalacturonan-I (RG-I) from the *gals* triple mutant and plants overexpressing *GALS1* in comparison to the WT. RG-I was enriched from alcohol insoluble residue (AIR) prepared from rosette leaf material of three to five four-week-old plants overexpressing *GALS1* under the control of the CaMV 35S promoter, the *gals1-1/gals2-1/gals3-1* triple mutant and WT control. The monosaccharide composition was measured by HPAEC-PAD. Values are the mean of three biological replicates \pm SD.

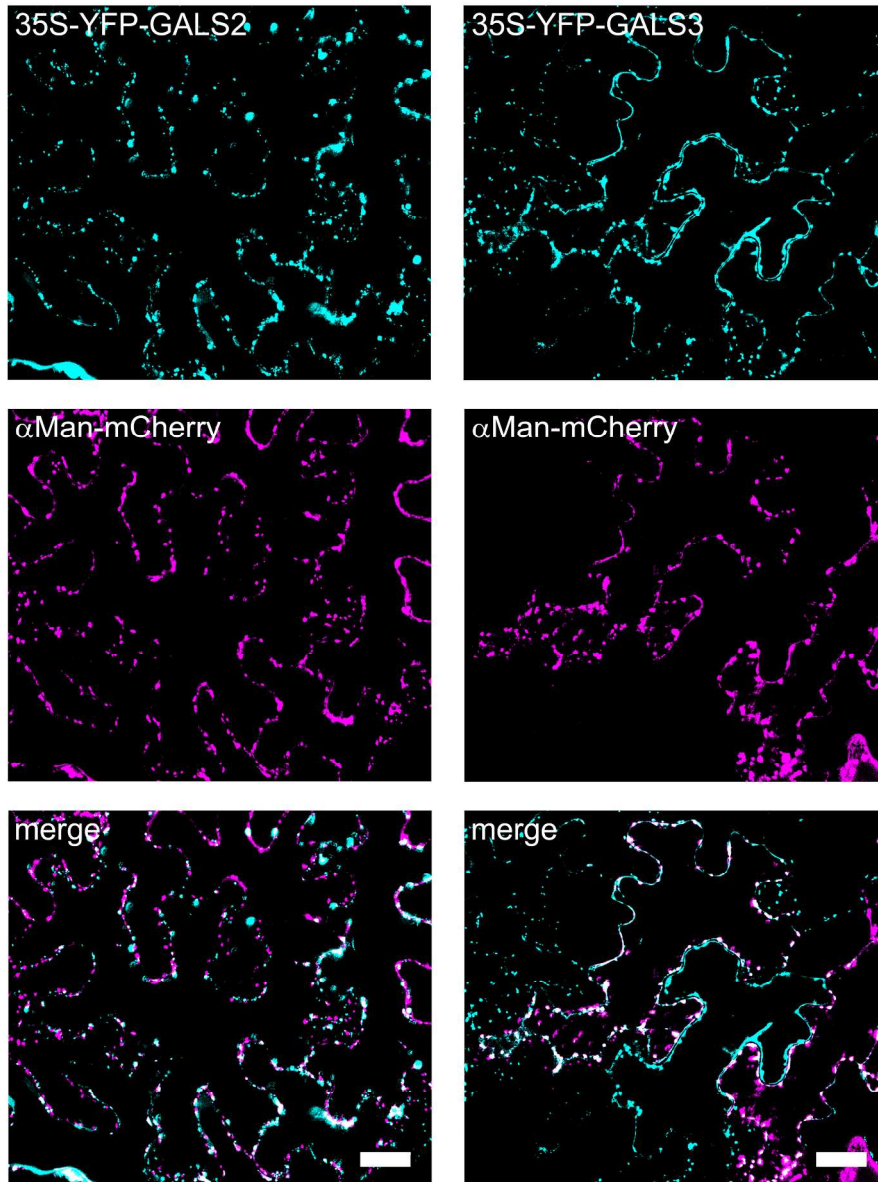


FIGURE 1 Sub-cellular localization of the GALS2 and GALS3 proteins. The coding sequences of the proteins were fused to YFP at their C-termini (first row) and compared to the Golgi marker α -mannosidase-I fused to mCherry (middle row). The merged signals (last row) confirm that both GALS2 and GALS3 co-localize with the Golgi marker. Scale bars are 25 μ m.

110x145mm (600 x 600 DPI)

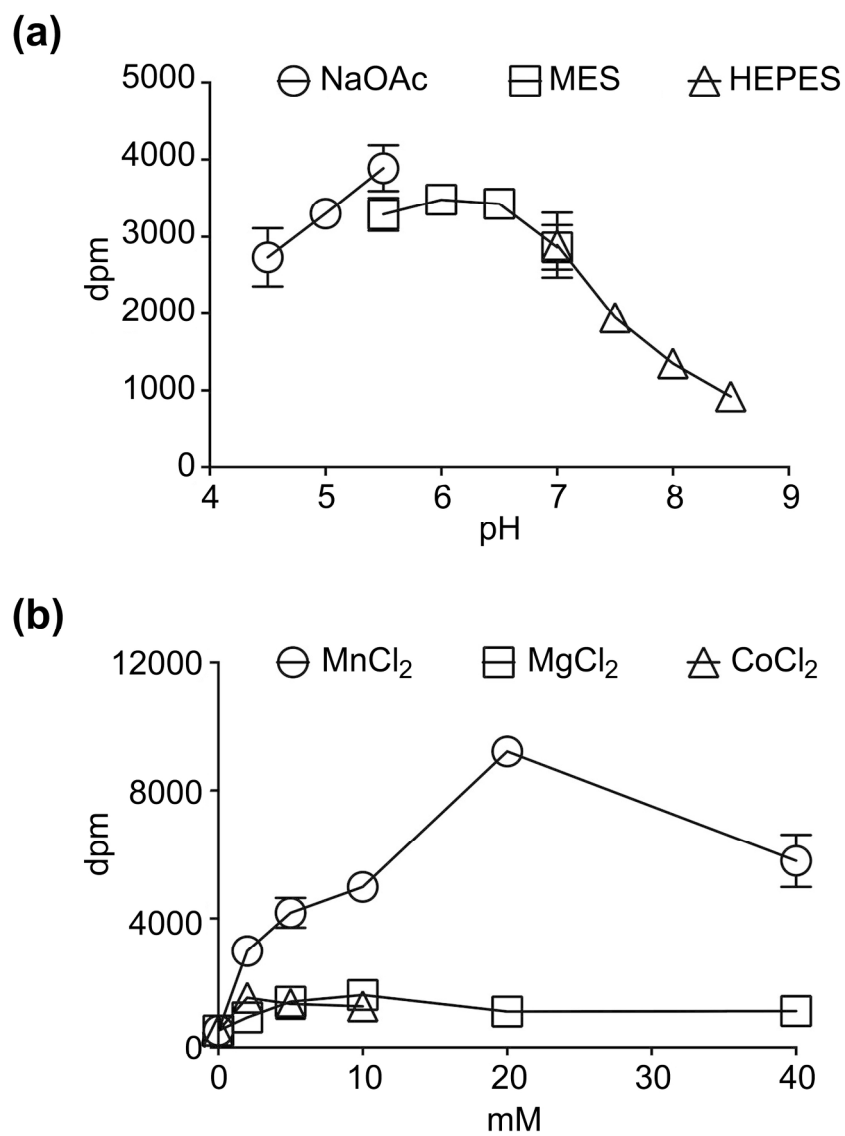


FIGURE 2 Enzymatic characteristics of the recombinant and affinity-purified YFP-GALS1 protein. (a) pH optimum (b) divalent cations. The data shows averages \pm SEM (n = 2).

98x115mm (600 x 600 DPI)

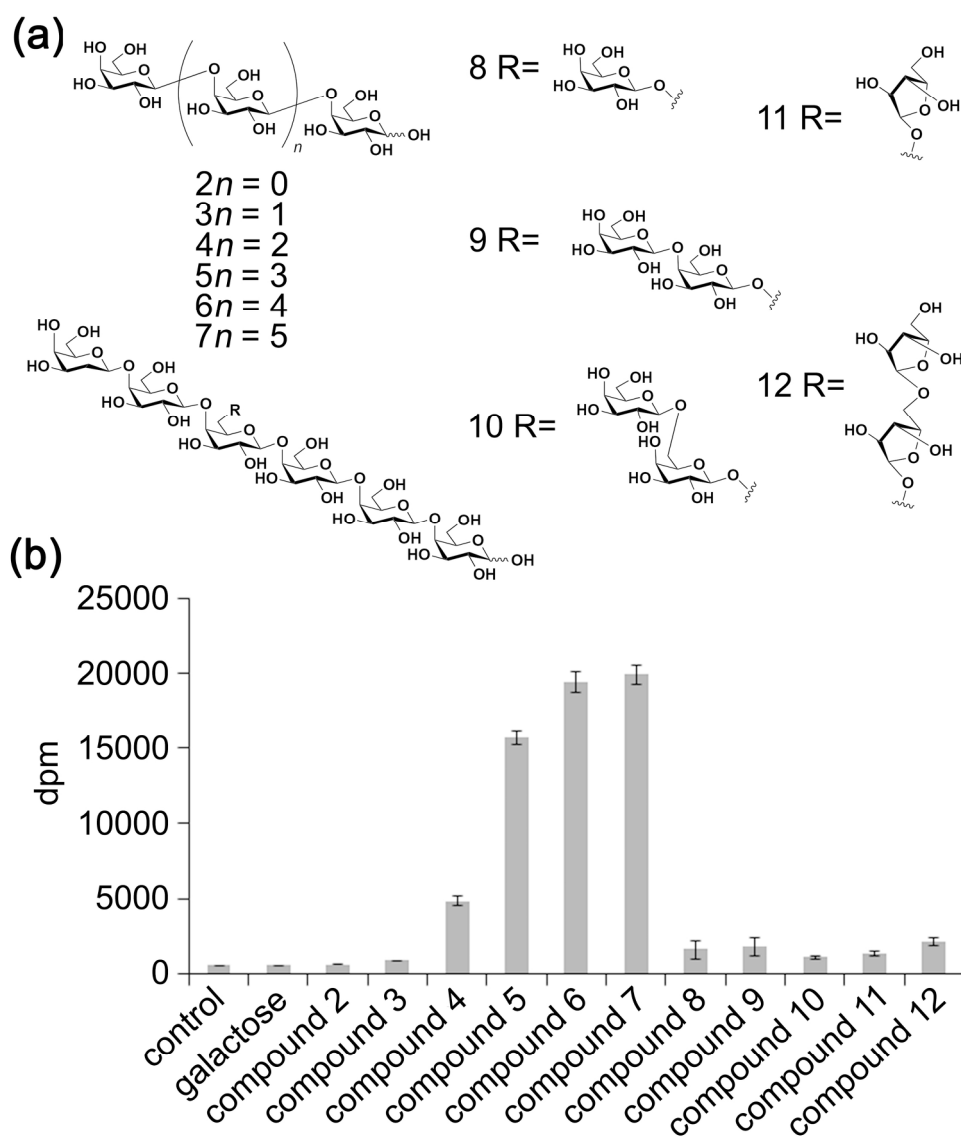


FIGURE 3 Activity of recombinant purified GALS1 protein probed with various acceptors. (A) Structures of galacto-oligosaccharides prepared by chemical synthesis. Galacto-oligosaccharides (compound) 2 to 7 are linear β -1,4-linked structures ranging from with galactobiose (compound 2) to galactoheptaose (compound 7). The remaining structures have a β -1,4-linked hexasaccharide backbone branched at the C6 position of the 4th Gal residue from the reducing end. Compounds 8 to 10 have Gal branches of DP=1 and 2, respectively, whereas 11 and 12 carry α -L-Ara branches of DP=1 and 2, respectively. (B) Galactan synthase (GalT) activity of recombinant and purified GALS1 protein transiently overexpressed in *N. benthamiana*. The GalT activity assays were performed with purified 35S-FLAG-GALS1 protein, UDP-[14 C]Gal and different exogenous unbranched acceptors and branched acceptors. Error bars are SEM ($n = 3$ biological replicates). Significant differences from control are indicated (T-test; *, $p < 0.05$; **, $p < 0.01$).

98x115mm (600 x 600 DPI)

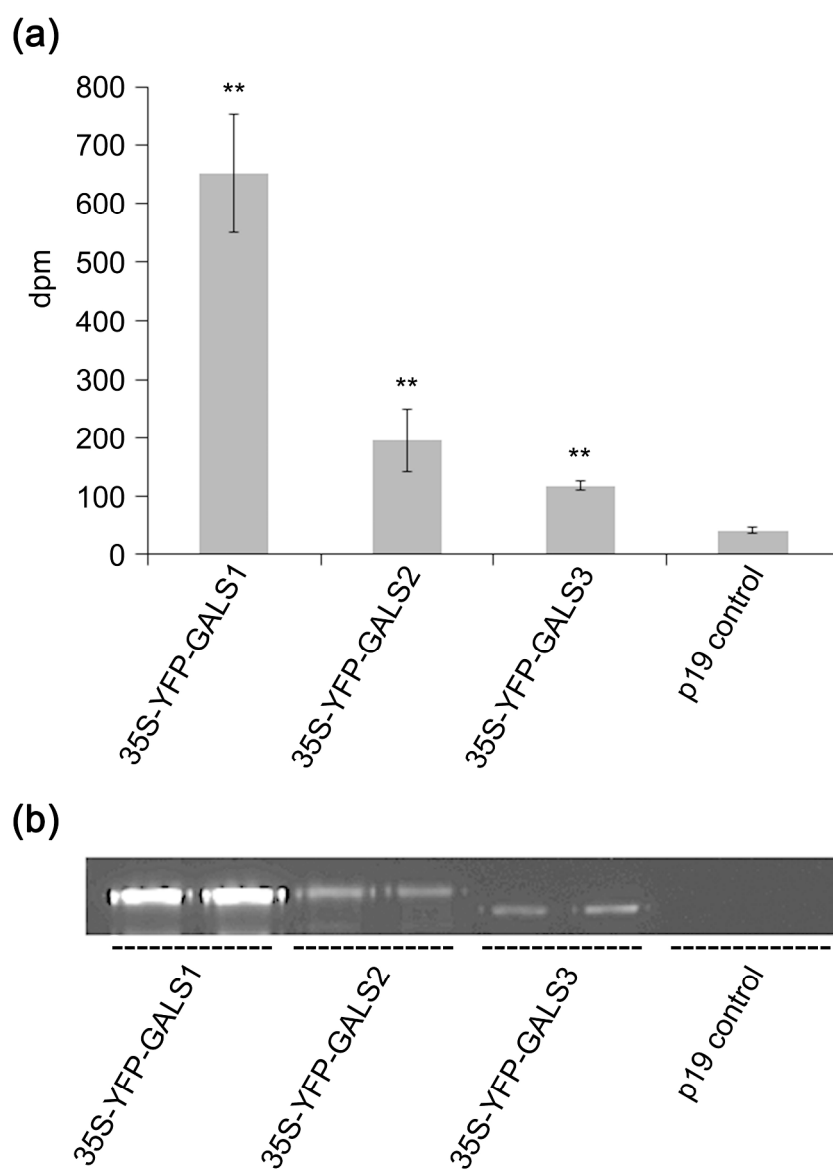


FIGURE 4 Galactan synthase activity of microsomal proteins from *N. benthamiana* overexpressing GALS1, GALS2 and GALS3. (A) [¹⁴C]Gal incorporation by microsomal membrane preparations without addition of exogenous acceptor. Plants infiltrated with *A. tumefaciens* containing 35S-FLAG-GALS constructs for GALS1, GALS and GALS3 respectively and p19 and plants infiltrated only with p19 were used as control. Error bars are SEM with n = 3 biological replicates. Significant differences from control are indicated (t-test; *, p < 0.05; **, p < 0.01). (B) Immunoblot analysis to assess GALS1, GALS2 and GALS3 protein abundance in the microsomal preparations used in (A).

113x151mm (600 x 600 DPI)

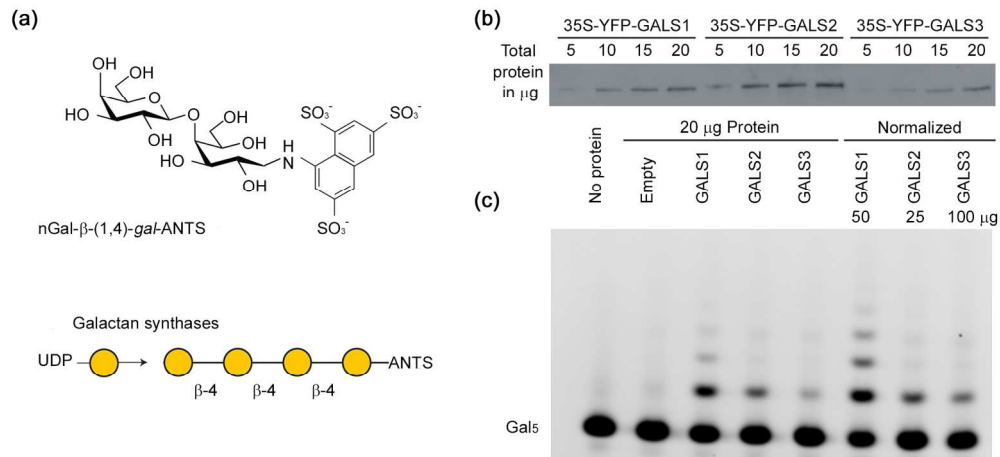


FIGURE 5 Fluorescent assay determining the activity of recombinant GALS proteins. (A) Schematic showing the chemically synthesized galacto-oligosaccharide acceptor reductively coupled with an ANTS fluorescent probe and addition of a Gal moiety from the UDP-Gal precursor onto the growing galacto-oligosaccharide chain as mediated by galactan synthases. (B) Immunoblot analysis to assess GALS1, GALS2 and GALS3 protein abundance in microsomal preparations from Arabidopsis plants expressing the three GALS proteins under the CaMV35S promoter. (C), GalT activity of the GALS proteins determined by carbohydrate gel electrophoresis (PACE) using galactopentaose-ANTS as acceptor and UDP-Gal as donor. Protein content was normalized to total microsomal protein or based on protein abundance as determined by immunoblotting.

169x78mm (300 x 300 DPI)

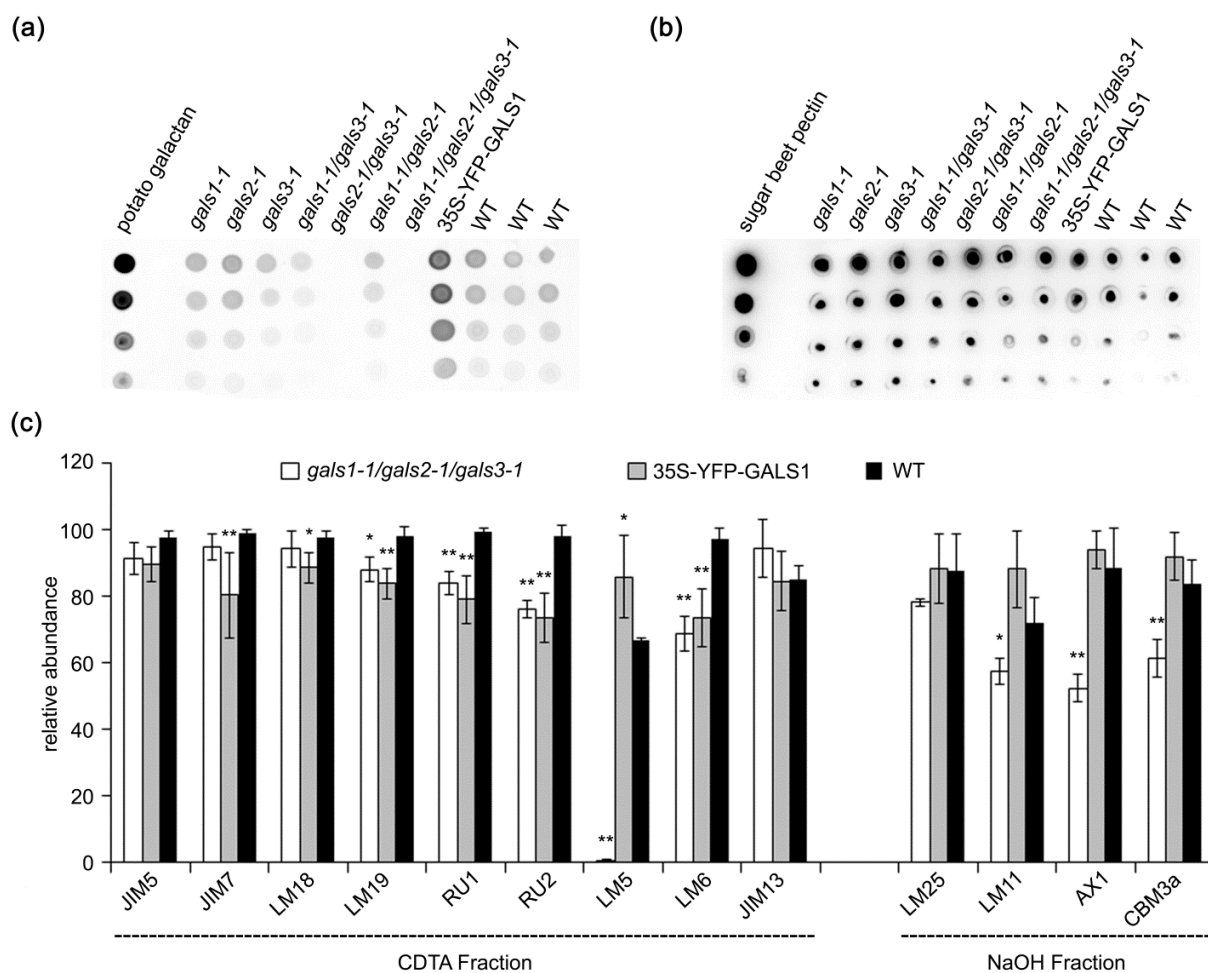


FIGURE 6 Immunodot blot assays of cell wall extracts isolated from Arabidopsis rosette leaves from mutant and WT plants. The extracts were probed with LM5 for (A) 1,4-galactan and (B) LM19 for homogalacturonan. (c) Microarray polymer profiling analysis with relative abundance of cell wall glycan epitopes in CDTA and NaOH-extracted fractions from alcohol insoluble residue (AIR). Mean and SD for spot signals (MSS) were obtained by probing microarrays with various antibodies recognizing the epitope of representative cell wall polymers (x axis) from four technical replicates with pooled material from eight plants. The highest MSS was set to 100 and all other values adjusted accordingly. Values significantly different from the WT are marked with asterisks (*, P < 0.05; **, P < 0.01; t test).

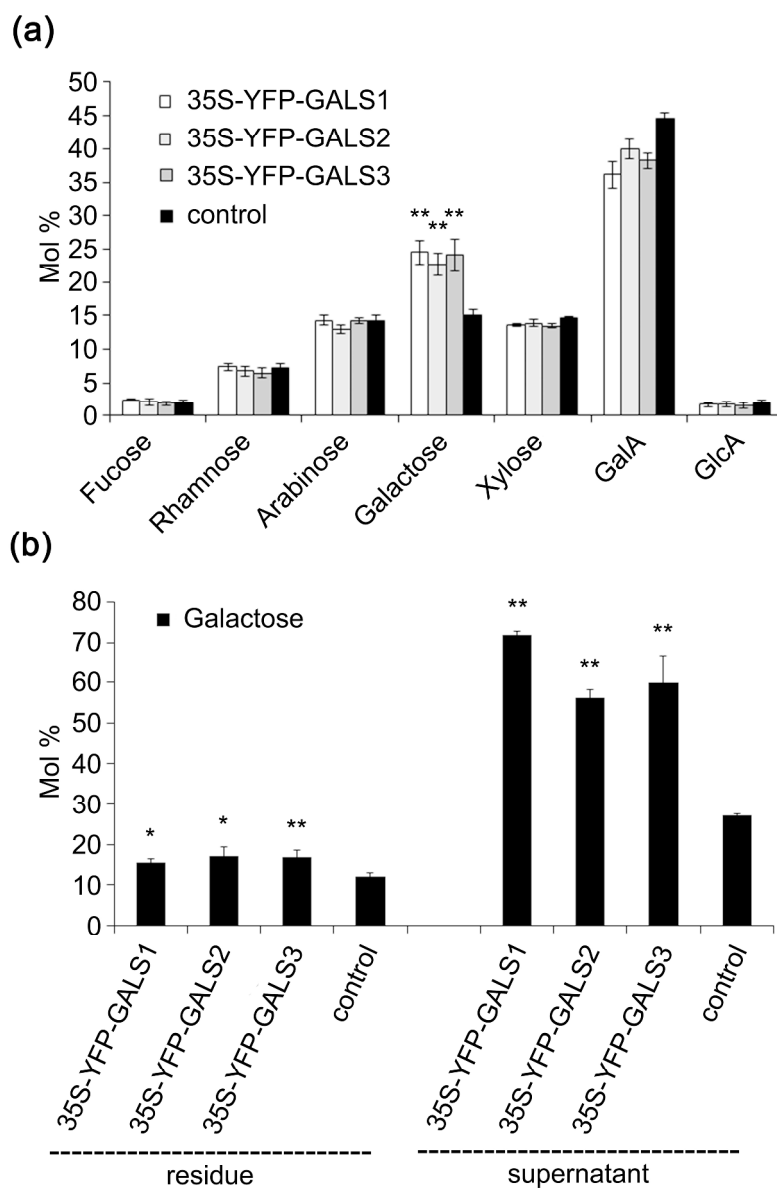


FIGURE 7 Analysis of the monosaccharide composition of leaves from six-week old plants overexpressing GALS1, GALS2 and GALS3 under the control of the CaMV 35S promoter in comparison to the WT. (A) Monosaccharide composition measured by HPAEC-PAD. Values are the mean of eight biological replicates \pm SD. (B) Galactose content of cell wall material derived from six-week old WT plants and plants overexpressing the GALS proteins after digestion with endo- β -1,4-galactanase. The supernatant was separated from the insoluble material (residue) and the amount of galactose was measured by HPAEC-PAD. Values are the mean of four replicates \pm SD. Values significantly different from the WT are marked with asterisks (*, $P < 0.05$; **, $P < 0.01$; t test).

126x188mm (600 x 600 DPI)

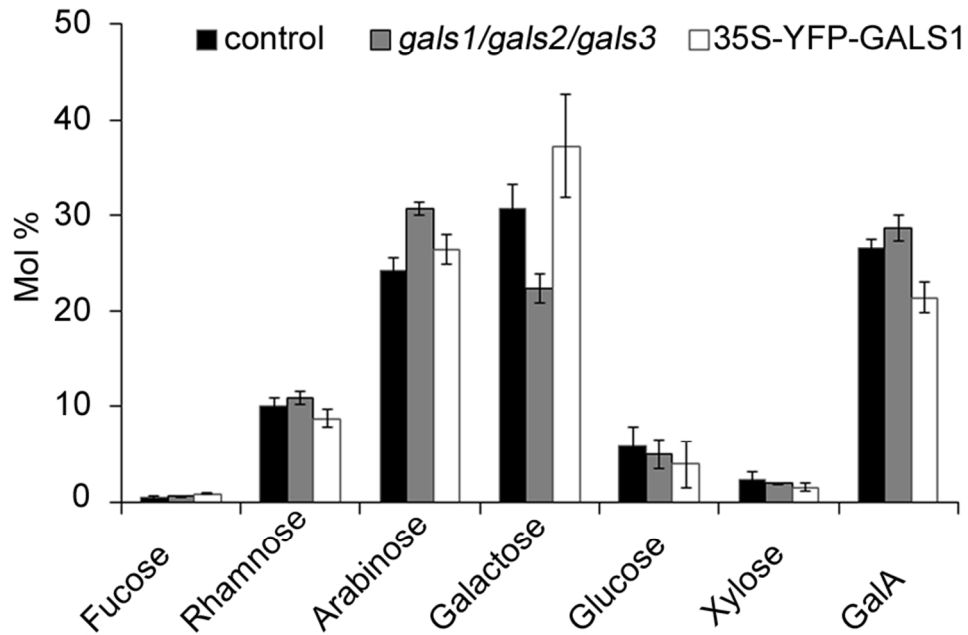


FIGURE 8 Analysis of the monosaccharide composition of rhamnogalacturonan-I (RG-I) from the *gals* triple mutant and plants overexpressing GALS1 in comparison to the WT. RG-I was enriched from alcohol insoluble residue (AIR) prepared from rosette leaf material of three to five four-week-old plants overexpressing GALS1 under the control of the CaMV 35S promoter, the *gals1-1/gals2-1/gals3-1* triple mutant and WT control. The monosaccharide composition was measured by HPAEC-PAD. Values are the mean of three biological replicates \pm SD.

84x57mm (300 x 300 DPI)